An Interactive Simulation of The Muscle Spindle

Oliver Stirling Schneider
Department of Computer Science
The University of British Columbia
Vancouver, BC, CA
oschneid@cs.ubc.ca

ABSTRACT
The muscle spindle is an important biological sensor, but is not yet completely understood. Recently, many mathematical and computational models have been developed to aid understanding of the processes that control the muscle spindle. I am implementing a recent model developed by Mileusnic et al. [9], which presents a single model to model primary and secondary afferent signals under various fusimotor drive states. After a brief overview of the muscle spindle's physiology and previous modeling attempts, I present an explanation of the algorithm. I then present my implementation efforts: a working Simulink implementation that produces output qualitatively similar to the original's. I also provide an interactive visualization of both the primary and secondary afferent signals, with fascicle length and static and dynamic fusimotor drives as input. Numerical limitations are briefly discussed, and future usability improvements are outlined.

Author Keywords
Muscle spindle; computational model; implementation; simulation.

ACM Classification Keywords
I.6.m. Simulation and Modeling: Miscellaneous

;

J.3 Computer Applications: Life and Medical Sciences

General Terms
Design; Documentation; Experimentation.

INTRODUCTION

The muscle spindle is a key organ for proprioception, the ability for the body to sense itself. In particular, the muscle spindle senses changes in the length of the muscle that surrounds it, which also helps infer changes in joint angles [5]. To better understand the mechanisms of the muscle spindle, several computational models have been developed (*e.g.*, [6, 7, 9, 3, 10, 1]). One of the most recent and comprehensive is the model developed by Mileusnic et al. [9]. Important features of this model include the correct description of partial occlusion between primary and secondary afferent signals under fusimotor drive, and a single set of parameters that describe muscle spindle activity under a wide range of circumstances.

I have implemented this model, and demonstrate results qualitatively similar to the output presented by Mileusnic et al. In addition, I have built an interactive application that allows users to learn about the model by effectively playing with the simulation inputs (spindle length and fusimotor drive), and view both afferent responses in real-time. Real-time implementation is not without its limitations; the model exhibits instabilities, which affect the accuracy of real-time display. These limitations are mentioned, but are not prohibitive to the end-goal of real-time interaction with the model.

In this work, I provide 4 main contributions. First, I provide a high-level summary of necessary background information to understand the model, including muscle spindle physiology and function, and a brief summary of Mileusnic et al.'s report on previous modeling efforts [9]. Second, I provide a description of the model's algorithm alongside my implementation details and design decisions. Third, I describe the results of my implementation, including the mentioned instabilities. Finally, I present an interactive system that allows users to play with the model in real-time.

BACKGROUND

The muscle spindle has been studied extensively, both in traditional medicine and through mathematical and computational models. Here I provide a summary of physiology important for understanding the model, and a high-level summary of previous modeling efforts discussed by Mileusnic et al. [9].

Muscle Spindle Physiology

The muscle spindle is a proprioceptive sensor located in the muscle. Several muscle spindles working together in every muscle provide important information about the length and rate of length change of the muscle,

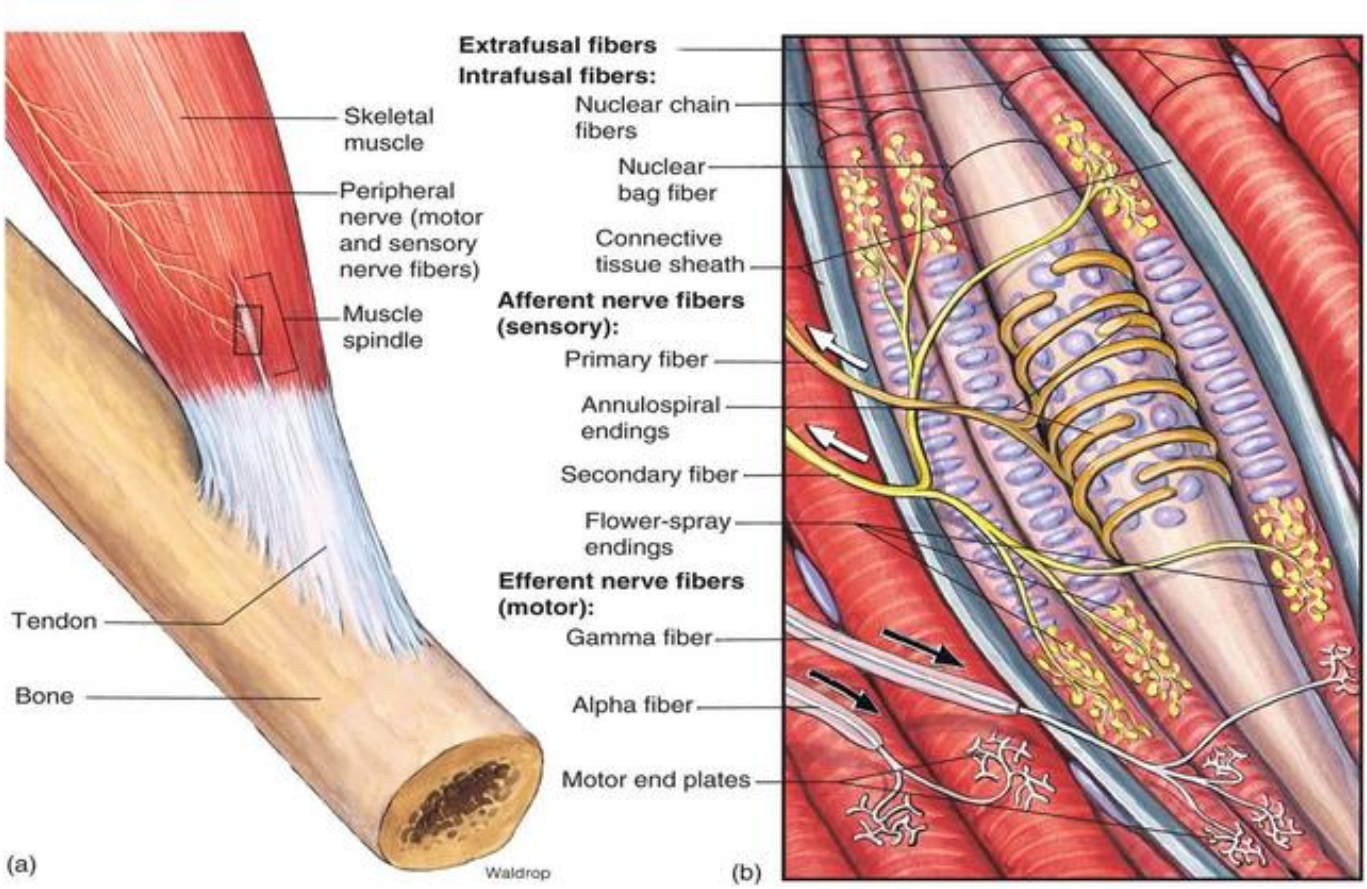

Figure 1: The muscle spindle location and anatomy [2].

from which the brain can infer corresponding information about joint angles. Throughout both the form and function of the muscle spindle, there is a division between these two types of information: static (of the muscle spindle's length) and dynamic (rate of change of the length). This duality is present in the two afferent signals, fusimotor drive (innervation of the intrafusal fibers), and form key structural components in the model proposed by Mileusnic et al. [9]. Please see Figure 1 for an image of the muscle spindle.

The muscle spindle is composed of specialized muscle fibers referred to as *intrafusal* fibers[1]. As with extrafusal fibers, intrafusal fibers can be contracted through innervation by motoneurons. While alpha motoneurons innervate extrafusal fibers, intrafusal fibers are innervated by beta and gamma motoneurons. There are three types of intrafusal muscle fiber, visible in Figure 2:

Dynamic nuclear bag fibers provide dynamic (rate of change) information about the muscle spindle's length. They are innervated separately from the static nuclear bag fibers and nuclear chain fibers. Information from these fibers only appears in the primary afferent signal. As a bag fiber, they have nuclei clustered in the middle to give the paunchy bag-like appearance. There are normally 2-3 bag fibers in a muscle spindle (divided into dynamic and static bag fibers) [5]. When modeled, these are referred to as $\texttt{bag}_1$ fibers. They are innervated by dynamic beta and gamma motoneurons.

Static nuclear bag fibers are another type of bag fiber, and are structurally similar to dynamic nuclear bag fibers. The difference is that these fibers provide information about the length that is robust to the rate of change (static information). As such, they provide information to both the primary and secondary afferent signals, and are innervated by static beta and gamma motoneurons. They are referred to as $\texttt{bag}_2$ fibers in models.

Nuclear chain fibers have a different appearance from the bag fibers, as the nuclei are spread throughout the fiber. A muscle spindle typically has about 5 chain fibers [5]. They provide static information to both primary and secondary afferent signals, and are innervated by static beta and gamma motoneurons.

[1] *cf. extrafusal* fibers, muscle fibers located outside the muscle spindle.

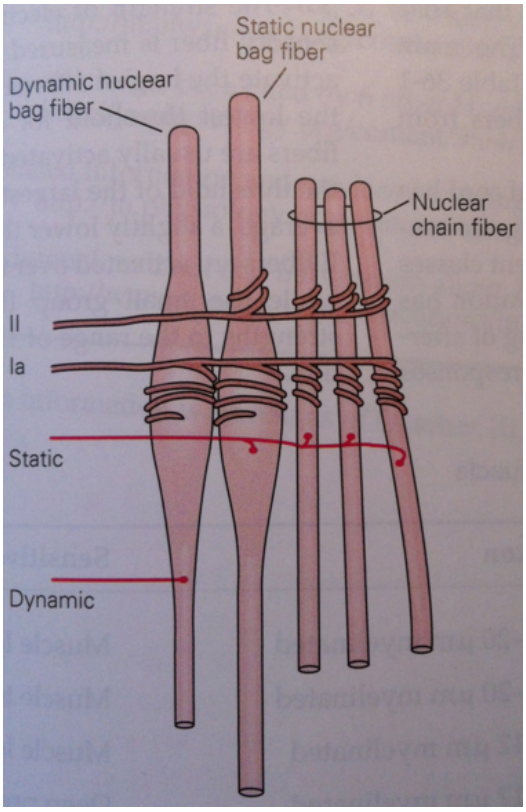

Figure 2: Intrafusal fibers [5].

Note that contraction of the intrafusal fibers differs from extrafusal fibers in two ways. First, the force generated by intrafusal fibers is much smaller than extrafusal fibers, and typically does not influence overall force generation in the muscle **[pending]**. Second, only the *polar regions* of the muscle fiber contract - the *sensory region* in the middle does not directly contract. The primary afferent signal includes transducers only in the sensory region, so it is only the stretch in this region that contributes to primary afferent firing. However, secondary afferent transducers straddle both the sensory and polar regions (see Figure 1), and the stretch of both regions contributes to the secondary afferent signal [9].

Because the contraction of the muscle spindle does not add to overall force generated by the muscle, scientists hypothesize that it is used to adjust afferent signals. By contracting the polar regions, the sensory reagion is stretched, which leads to either an increased likelihood of the afferent firing, or an increased firing rate [5]. The reason for this is being actively discussed in the community and remains controversial, but one hypothesis is that contraction of the intrafusal fibers allows afferent signals to operate as an optimal transducer by adjusting the range of lengths for which it is sensitive [9]. One of the primary motivations in the development of Mileusnic et al's model is to investigate the role of fusimotor drive and test this hypothesis.

The output of the muscle spindle is provided in two afferent signals: one primary (Ia signal) and one secondary (II signal)[2]. The primary afferent signal provides both static and dynamic information, while the secondary afferent signal provides only static information. Thus, the brain is able to use the two signals to infer static and dynamic information individually. Firing rate is linear-proportional to the length, but is heightened in the primary afferent during stretch (the dynamic stage of the system) [5]. See Figure 3 for an example of the primary afferent signal.

The primary signal produces both static and dynamic information because it has sensors on all intrafusal fibers, while the secondary afferent has sensors on all but the dynamic nuclear bag fiber (which produces dynamic information). See Figure 2.

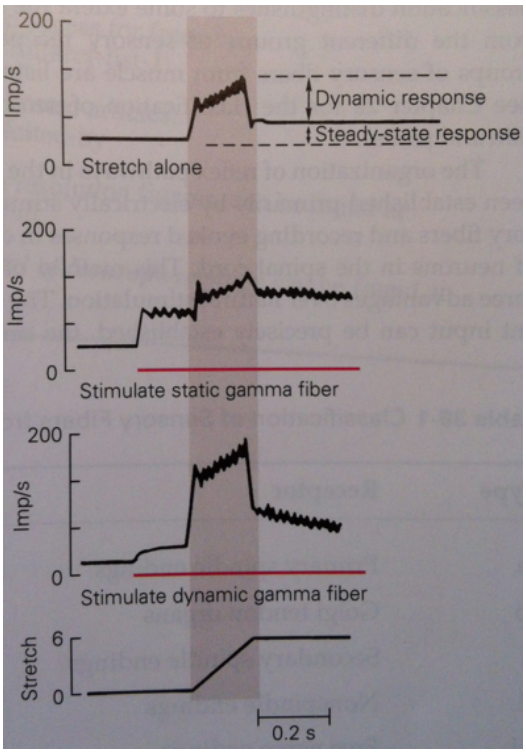

Figure 3: Response of the primary (Ia) afferent signal in different fusimotor drive states [5].

Previous Modeling Efforts

Because of its importance in sensorimotor systems, the muscle spindle has a long history of mathematical and computational models (as far back as 1968 [1]). One of

[2]The naming convention for these signals is derived from classification of axon diameter in neurons producing an afferent signal from muscles. For example, the Golgi tendon organ has the same axon diameter as the primary afferent signal in the muscle spindle (12-20μm), and its signal is referred to as the Ib signal [5].

the most important models is Hasan's [3], which presented mathematical descriptions of anatomical components, provided a simple but accurate description of spindle afferent under fusimotor drive, and has been widely adopted and tested [9]. However, it has a rigid structure - the full parameter set needs to be changed for each fusimotor state, and thus the direct dynamics of efferent activity is not captured. As well, it suffers error in the initial burst of afferent activity under repeated stretching.

Schaafsma et al. [10] provide a next major step, capturing fusimotor effects but only producing the primary afferent signal [9]. This was also anatomically inspired, with two nuclear bag fiber submodels ($\texttt{bag}_1$ and $\texttt{bag}_2$ for dynamic and static, respectively). Schaafsma et al.'s model performed well for ramp-and-hold stretches, but underestimated afferent activity induced by sinusoidal stretching. This model uses a complete occlusion[3] of afferent signals rather than partial occlusion (which was explained in 1997-2001), and was expanded in 1995 to include a chain fiber submodel [11].

Maltenfort [7] modeled fusimotor effects and partial occlusion with a black-box model rather than a structurally anatomical one [9]. Maltenfort's model captures the partial occlusion effect, but has limited performance, again highlighted with sinusoidal stretching.

Lin and Crago [6] modeled both intrafusal and extrafusal fibers. Their model of intrafusal force generation is similar to the one implemented by Mileusnic et al. [9]. However, their model used complete occlusion of afferent signals, and was not throughly validated under both dynamic and static fusimotor drive.

With this history highlighted, the advantages of Mileusnic et al. are clear: anatomical structure, output of both afferent signals in all states of fusimotor drive, modeling of partial occlusion, and a single set of parameters drawn from the literature (as well as ones determined during development). Their validation includes both ramp-and-hold signals and sinusoidal signals for stretching. Limitations include the lack of an initial burst effect present in models as early as Hasan [3].

IMPLEMENTATION

Overall, the muscle spindle model receives fascicle length and static and dynamic fusimotor drives as input. It produces primary and secondary afferent signals as output. I have chosen to implement the model in Matlab Simulink [8], the same system in which Mileusnic et al. implemented the original model. The architecture of my implementation closely follows the dynamical system outlined in the source paper, and as such mirrors the

[3]The primary afferent signal is not independent of the secondary afferent signal. A stronger secondary afferent signal will reinforce the primary signal, to the point where the primary signal is almost entirely composed of the secondary signal. Complete occlusion is a simplification that simply chooses the stronger of the two signals for the primary afferent neuron's output.

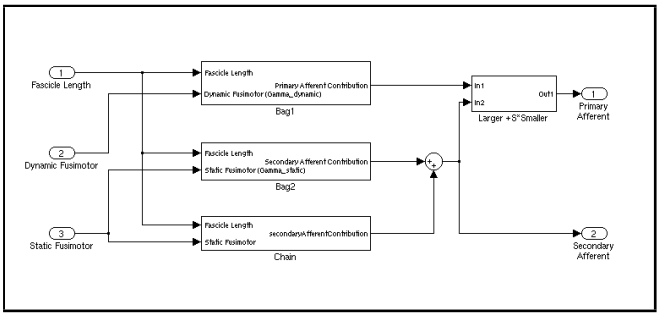

(a) My implementation in Matlab/Simulink.

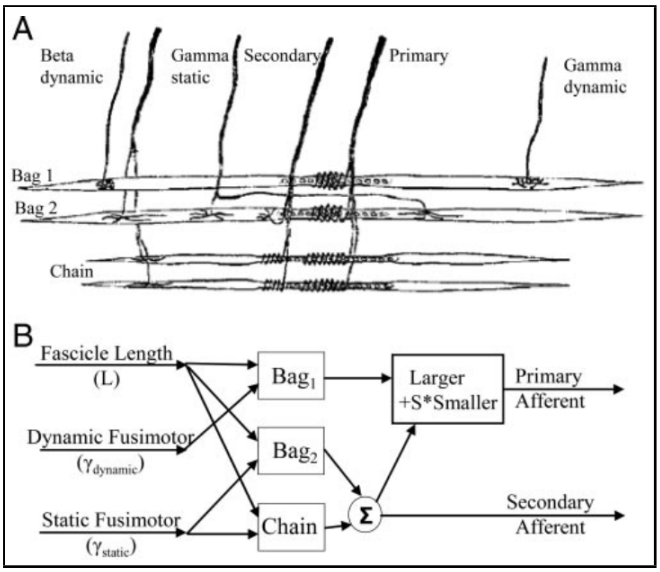

(b) Original architecture and spindle anatomy [9].

Figure 4: Muscle spindle architecture.

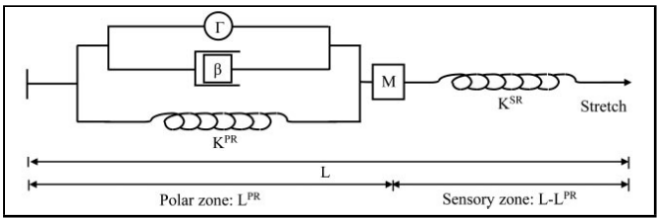

Figure 5: Intrafusal fiber model [9].

physical anatomy of the muscle spindle. In particular, there are three subsystems that implement sets of intrafusal muscle fibers, $\texttt{bag}_1$, $\texttt{bag}_2$, and `chain`. The system architecture my implementation can be seen alongside the original architecture and biology in Figure 4.

The model uses similar submodels for each types of intrafusal fiber, aggregated by type (for example, the response of all chain fibers is in a single `chain` submodel). Each intrafusal fiber is implemented as a Hill-type model [4]. The intrafusal fiber model simulates noncontracting sensory regions as a passive spring, and the contracting polar regions as a spring with a damping component (β) and a non-linear force generating component to represent innervation (Γ). The length of these two sections is the total length of the muscle spindle, provided as input. Thus, after calculating the length of the polar region, the model uses this to find the length of the sensory region and produces firing rate proportional to this section's length. The force generating section uses biochemical equations to generate contraction. Mass, spring constants, damping coefficients, force-generating coefficients, and other constants are defined for each intrafusal fiber type based on the literature (data is from a lower-limb feline muscle spindle). Please see Figure 5 for the basic intrafusal fiber model.

Next, equations for tension in both components are manipulated into a second-order differential equation of tension in terms of fascicle length. Stretch (T/K_{sr}, where T is tension and K_{sr} is the sensory zone spring constant) is then used as input in two impulse-generating centers. Exact mechanisms of the muscle spindle's impulse generation are not known; the literature suggests that there are two. This model assumes that one is located on the $\texttt{bag}_1$ fiber, and the other generates impulse from the $\texttt{bag}_2$ and `chain` fibers. Finally, the partial occlusion of afferent activity is represented by the common belief of the primary afferent afferent being dominated by the stronger of the two impulse generators. I have implemented these equations as Simulink blocks.

VALIDATION

Because my focus is on the interactive application, a thorough validation of my implementation is beyond the scope of this project. However, throughout development I have been comparing output to results presented in the paper. I have replicated the ramp-and-hold results under fusimotor drive (Figure 3 in [9]). As Mileusnic et al. compare their results to experimental data qualitatively, so do I compare my results qualitatively with theirs. These results examine primary afferent firing, but secondary afferent firing is similar. I have used a fixed-step solver (`ode3`, Bogacki-Shampine) with a relative error of 1×10^{-3}, the same as that in my interactive application. Length begins as $0.95L_0$, then ramps after 1 second to $1.08L_0$ with varying slope. Total simulation time is 3.3 seconds.

Qualitatively, my results are very similar to the output presented by Mileusnic et al., but there are two differences (see Figure 6). First, the model begins by producing a negative afferent signal that slowly converges to 0. I believe that this is a result of poor initial conditions for the tension calculation. However, my attempts to fix this (by setting $\dot{L} = \ddot{L} = 0$ and solving) did not fix it.

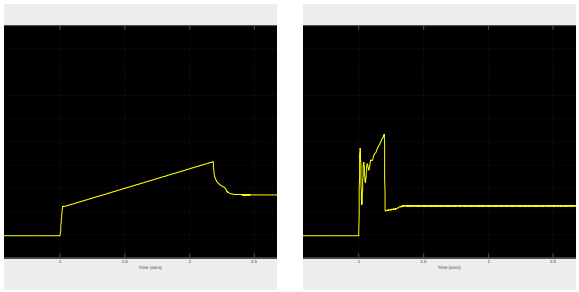

(a) Slow ramp (5 mm/s) (b) Medium ramp (30 mm/s)

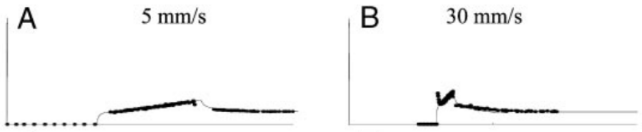

(c) Results reported by [9]

Figure 6: Primary afferent results from a ramp-and-hold length signal with no fusimotor drive.

The second and more critical problem produces oscillation when the ramp begins. Although less of a concern when there is no fusimotor drive (6a), this becomes more exaggerated with a steeper ramp (6b). I suspect that the tension calculation is extremely stiff because of the coupled springs, the coefficient of asymmetry (which changes depending on whether the spindle is stretching or compressing), and the involvement of the first and second derivatives of length. Variable-step solvers and stiff solvers produce similar results when given a minimum step size of 1×10^{-13} or greater, and freeze when the ramp starts otherwise. The model *MuscleSpindleTest.mdl*, provided with my source code, was used to create these. When running this model, be sure to set the solver in *MuscleSpindle.mdl* to be the same as that in *MuscleSpindleTest.mdl*, and the solver in *ContinuousDetectIncrease.mdl* to be fixed-step or variable-step discrete (as appropriate).

INTERACTIVE SYSTEM

To facilitate understanding of the muscle spindle, especially with those encountering it for the first time, I have implemented a real-time interactive application that allows the user to manipulate input and view output (Figure 7). This application uses Matlab's Graphical User Interface (GUI) toolkit as a wrapper around a simple Simulink model, `MuscleSpindleGUIModel`, that drives

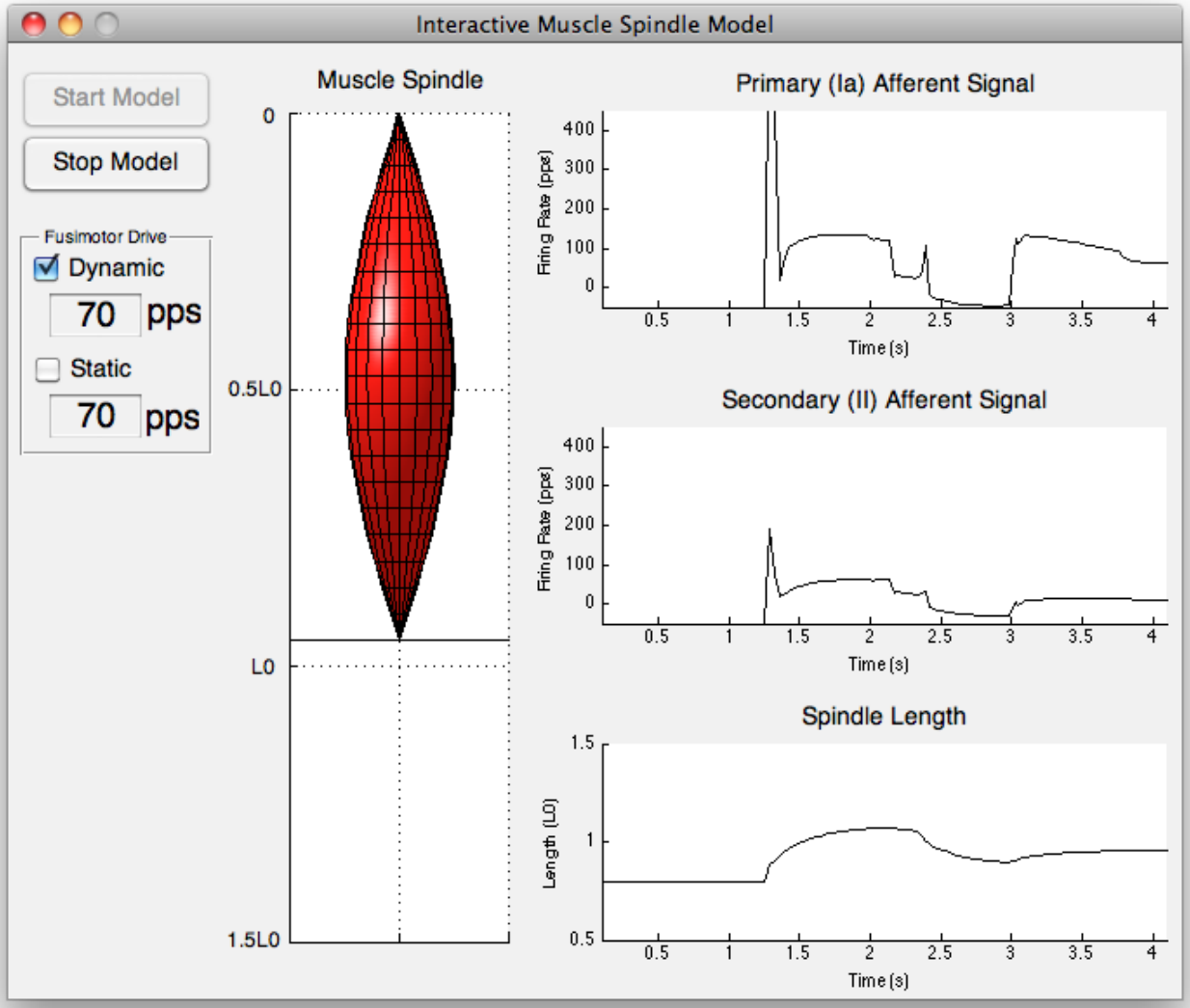

Figure 7: Screenshot of the interactive application.

the model.

The user can start or stop the model using buttons at the top left. Execution time is infinite, and the model continues running until stopped. Checkboxes allow the user to enable or disable both static and dynamic fusimotor drive. Innervation levels can also be manipulated using editable text boxes. Fusimotor drive is specified in pulses-per-second (pps).

The muscle spindle's length is controlled through a rudimentary visualization in the center of the interface. To prevent discontinuities in the length's value, the user specifies a target length by clicking (and, if desired, dragging) on the visualization. A Potential-Integral-Derivative (PID) controller uses the error between the spindle's length and the target length to control the length's first derivative (chosen over the second derivative for responsiveness). This is meant to feel like a direct manipulation of the muscle spindle. Length is specified in units of L_0, the spindle's rest length. Target length is restricted to being between $0.8L_0$, slack length, and $1.4L_0$, at which the afferent firing rates tend to exceed the scale. The visualization is created through a modified cylindrical Matlab surface with Phong lighting.

Primary and secondary afferent signals are displayed at the right with a scrolling axis. The axis limits ($-50 \leq y \leq 450$, 4 seconds of time) are given approximately the same axis limits as the paper's outputs for qualitative comparison. A signal of length is presented below for comparison.

To execute in real-time, the model uses a fixed-step solver (`ode3`, Bogacki-Shampine, with a relative error of 1×10^{-3}), and is thus not as accurate as might be possible in non-real-time. However, the GUI updates the signals and spindle visualization at the low rate of 10Hz[4], and so many of the instabilities are not sampled at a high enough rate to be displayed. The low update rate counteracts instabilities to give an intuitive and smooth signal suitable for interaction and exploration.

Execution Instructions

To run the interactive application, Matlab and Simulink are both required. Open the file *MuscleSpindleGUI.m* with Matlab, and run. It will automatically load the model as long as all files are found on the Matlab path. Please ensure that the model's solvers are the same in *MuscleSpindleGUIModel.mdl*, *MuscleSpindle.mdl*, and *ContinuousDetectIncrease.mdl*.

Planned Improvements

Due to time constraints, there are several changes that can be made to improve usability. There are several minor issues that were triaged during GUI polishing: limitations on spindle length value should be displayed visually (*e.g.*, greyed out); the spindle visualization should be entirely visually disabled when the model isn't running, as it does not accept input; and the fusimotor drive should be implemented as sliders to restrict users to a range (between 0 and the saturation point of 100 for bag fibers, and 150 for chain fibers).

I can substantially improve the model with a better visualization of the muscle spindle. With a representation of each anatomical component of the muscle spindle, users can understand the internal mechanisms intuitively. The controls for fusimotor drive can visibly connect to intrafusal fibers. With some minor changes to the model, the lengths for the polar and sensory regions could be captured independently. This would allow a visual representation of the intrafusal fibers being innervated when fusimotor drive is changed.

[4]MatLab is drawing the lines with the CPU, not the GPU. Update rates of 20 and 30Hz seemed to operate too slowly to be compelling, although the system could be adjusted.

CONCLUSION

In this work, I have presented the implementation of a computational model of the muscle spindle. I have provided necessary background, an explanation, and a brief validation for the model. Validation revealed that the model output is qualitatively very similar to that achieved in the original model implementation, but with some initial value and oscillation problems. I have also presented an interactive application that allows users to play with the muscle spindle to gain an intuitive understanding. With planned improvements, such as an anatomically-correct visualization, this could be a valuable tool for learning about the muscle spindle.

ACKNOWLEDGMENTS

A big thank you to Dr. Pai for his suggestions, guidance, and feedback during this term project.

REFERENCES

1. Crowe, A. A mechanical model of the mammalian muscle spindle. *Journal of Theoretical Biology 21*, 1 (Oct. 1968), 21–41.
2. Fox, S. I. *Human Physiology*. McGraw-Hill Education, 2004.
3. Hasan, Z. A model of spindle afferent response to muscle stretch. *Journal of Neurophysiology 49*, 4 (1983), 989–1006.
4. Hill, D. K. Tension due to interaction between the sliding filaments in resting striated muscle. the effect of stimulation. *J. Physiol. 199*, 3 (Dec. 1968), 637–684.
5. Kandel, E. R., Schwartz, J. H., and Jessell, T. M. *Principles of Neural Science*, 4th ed. McGraw-Hill, 2000.
6. Lin, C.-C. K., and Crago, P. E. Structural Model of the Muscle Spindle. *Annals of Biomedical Engineering 30*, 1 (Jan. 2002), 68–83.
7. Maltenfort, M. G., and Burke, R. E. Spindle model responsive to mixed fusimotor inputs and testable predictions of beta feedback effects. *Journal of neurophysiology 89*, 5 (May 2003), 2797–809.

8. Mathworks Inc. MATLAB R2012a, 2012.

9. Mileusnic, M. P., Brown, I. E., Lan, N., and Loeb, G. E. Mathematical models of proprioceptors. I. Control and transduction in the muscle spindle. *Journal of neurophysiology 96*, 4 (Oct. 2006), 1772–88.

10. Schaafsma, A., Otten, E., and Van Willigen, J. D. A muscle spindle model for primary afferent firing based on a simulation of intrafusal mechanical events. *J Neurophysiol 65*, 6 (June 1991), 1297–1312.

11. Scheepstra, K., Otten, E., Hulliger, M., and Banks, R. Modeling of chaotic and regular Ia afferent discharge during fusimotor stimulation. *Alpha and Gamma Motor Systems* (1995), 325–327.